Appl. Phys. B 65, 545–548 (1997)

Applied Physics B Lasers and Optics

Optical transient bleaching/absorption of surface-oxidized $CuInS_2$ nanocrystals

K.V. Yumashev[1], A.M. Malyarevich[1], P.V. Prokoshin[1], N.N. Posnov[1], V.P. Mikhailov[1], V.S. Gurin[2], M.V. Artemyev[2]

[1] International Laser Center, Belarusian State Polytechnical Academy, 65 F. Skaryna Ave., Bld. 17, 220027 Minsk, Belarus
(Fax: +375 /17-2326 286, E-mail: yumash_zone18@infra.belpak.minsk.by)
[2] Physico-Chemical Research Institute, Belarusian State University, 14 Leningradskaya Str., 220080 Minsk, Belarus

Received: 7 January 1997/Revised version: 16 April 1997

Abstract. The optical transient bleaching and induced absorption of oxidized $CuInS_2$ nanocrystals in a polymer film have been studied with the picosecond pump-probe technique. The oxidized $CuInS_2$ nanocrystals have an additional absorption band with a peak at 1.03 eV, which is bleached under picosecond excitation. Rapid ($\sim$ 50 ps) trapping into midgap surface states results in long-lived ($\gg$ 300 ps) bleaching and induced absorption features. A schematical energy-level diagram for oxidized $CuInS_2$ nanocrystals is given based on the experimental results.

PACS: 42.55 P; 42.70

Nanometer size semiconductor crystals have recently been extensively studied [1–8] because, in addition to a fundamental interest in their material properties they have been used as nonlinear optical devices [9–11]. A number of studies have been directed toward the optical behavior of chemically modified semiconductor nanocrystals [12–14]. The presence of the nanocrystal surface as a boundary and source of surface states makes the optical properties of nanometer-size crystals highly sensitive to chemical treatments. In this paper, we report the results of photoluminescence and picosecond (ps) pump-probe measurements on oxidized $CuInS_2$ nanocrystals ($CuInS_2$ NCs).

1 Experiment

$CuInS_2$ NC and oxidized $CuInS_2$ NC samples used in this study were synthesized in a poly[vinylalcohol] (PVA) polymer film by the following procedure. The $CuInS_2$ colloid was prepared from solution containing Cu(I) and In(III) by reaction with gaseous H_2S. PVA was used as a stabilizer of the colloids and film-forming material. To generate oxidized $CuInS_2$ NCs, the colloid was aged for about 10 days, changing color from brown to darkgreen. The aged colloids were also deposited and dried on a glass plate. The resultant $CuInS_2$ NC and oxidized $CuInS_2$ NC films were about 80 μm thick. The film samples prepared by the above method were stable, and their optical characteristics did not change throughout a year under the ambient conditions.

The X-ray diffraction data of $CuInS_2$ NCs on the PVA film were obtained using a universal Roentgen Diffractometer HZG 4 (produced by Freiberger Präzisionsmechanik) with CuK_α radiation and a Ni filter ($\lambda = 0.154$ nm). The X-ray diffractogram shown in Fig. 1a can be clearly attributed to the $CuInS_2$ chalcopyrite lattice (I42d spatial group) after comparison with the data in Fig. 1b. The size of the nanocrystals was determined using a transmission electron microscope with a resolution of $\sim$ 1 nm. The samples had a mean nanocrystal radius of 3 nm with a deviation ranging from 2 to 5 nm. The photoluminescence was excited by the 514.5-nm (2.41-eV) line of a continuous-wave Ar^+ laser and recorded at 10 K by a spectrometer with an optical multichannel analyzer system. In the pump-probe experiments, we have used the 15-ps duration pulses at 1.08 μm (1.15 eV) as a pump beam and the picosecond white-light continuum generated in a D_2O cell as a probe beam. An optical multichannel analyzer with two photodiode arrays as detectors was used to record the differential absorption spectra which were defined as $\Delta OD(\lambda) = -\lg[T(\lambda)/T_0(\lambda)]$, where $T_0(\lambda)$ and $T(\lambda)$ are the transmission spectra of the probe beam in the absence and presence of the pump beam, respectively. Negative magnitudes of ΔOD correspond to bleaching, and positive ones to induced absorption. The spot radius of the pump beam on the sample was $\sim$ 1 mm; excitation intensity was $\sim$ 1 GW/cm^2. Absorption changes were measured in the spectral region of 480–880 nm at room temperature and were temporary (the oxidized $CuInS_2$ NC sample returned to its initial absorption state).

2 Results

Curve (1) in Fig. 2 is the absorption spectrum of the $CuInS_2$ NC sample. It shows that the bound-exciton [12] (electron-hole pair confined to a nanocrystal) absorption appears as a broad shoulder mainly because of size inhomogeneity and phonon broadening. The exciton absorption peak at 1.78 eV (determined from the second derivative of the absorption spectrum and marked as a vertical bar in Fig. 2) is shift-

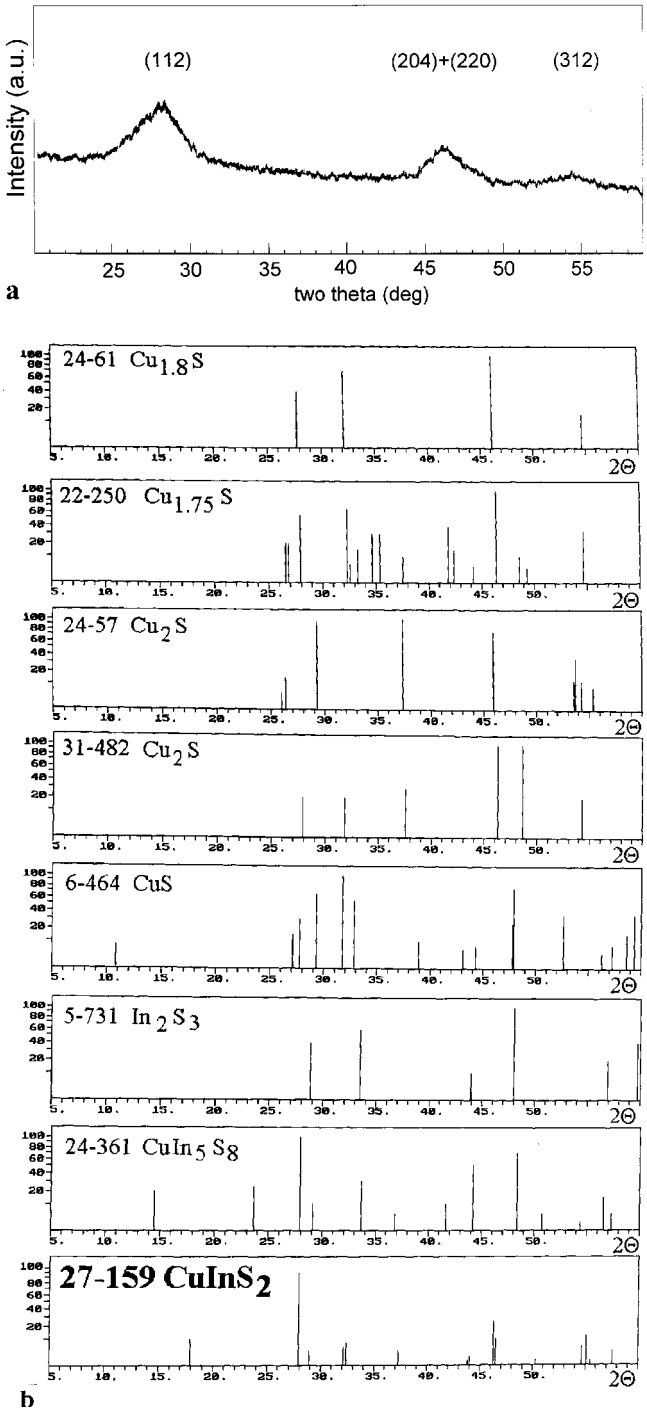

Fig. 1. a The X-ray diffraction data of the solid phase in the films investigated that were associated with ultrafine $CuInS_2$ particles. PVA film. Numbers in parentheses are assignments to the reflections in the $CuInS_2$ chalcopyrite lattice. **b** Comparison of JCPDS data for a set of compounds that are probable products under the synthesis of $CuInS_2$ allows conclusions as to formation of the chemical form $CuInS_2$. Numbers on diagrams denote the corresponding entry in the JCPDS catalogue

ed by 0.25 eV relative to the band gap of bulk $CuInS_2$ (1.53 eV) [15]. The blue shift ΔE is explained by the strong-quantum confinement model (with $R/a_B \leq 2$) [16], according to which:

$$\Delta E = h^2\pi^2/2\mu R^2 - 1.786e^2/\varepsilon R - 0.248E_{Ry}\,, \qquad (1)$$

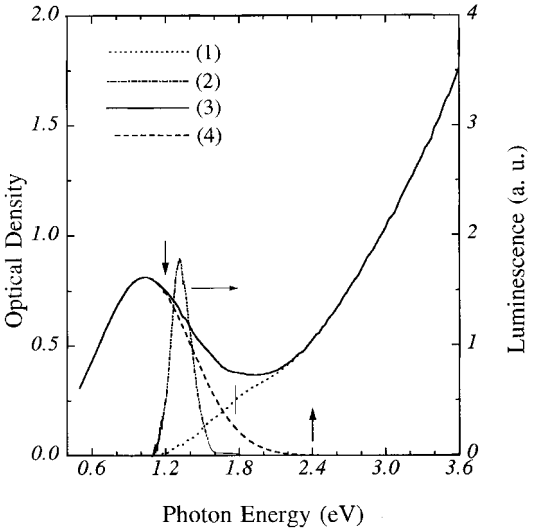

Fig. 2. The absorption spectra of (1) $CuInS_2$ NCs and (3) oxidized $CuInS_2$ NCs in a PVA film. *Dashed curve* (4) represents the absorption obtained by subtracting curve of absorphon (1) from absorption curve (3). The *arrows* [(↓) and (↑)] are markers for positions of pump photon energies in pump-probe and photoluminescence experiments, respectively. Curve (2) is the photoluminescence spectrum of $CuInS_2$ NCs in a PVA film taken at a temperature of 10 K

where R is the radius of the nanocrystals, a_B the exciton Bohr radius, $\mu = (1/m_e^* + 1/m_h^*)^{-1}$ the reduced mass, $m_e^*(m_h^*)$ an effective mass of the electron (hole), E_{Ry} the Rydberg energy, and ε a dielectric constant of the semiconductor. The values of $m_e^* = 0.16m_o$, $m_h^* = 1.3m_o$, $\mu = 0.14m_o$, $\varepsilon = 8.5$, $E_{Ry} = 26.9$ meV, and $a_B = 3.2$ nm that correspond to bulk $CuInS_2$ are adopted for the calculation [17, 18]. (1) explains the experimental blueshift, assuming that the radius of the nanocrystals is 2.7 nm. This value agrees well with the mean radius of 3.0 nm determined by transmission electron microscopy. The photoluminescence spectrum of the $CuInS_2$ NC sample consists of a broad band centered at 1.32 eV [curve (2) in Fig. 2]. The photoluminescence peak has 0.46 eV less energy than the exciton absorption peak (1.78 eV). Such photoluminescence is most likely due to radiative recombination from deep surface states [19, 20] observed for many types of film and glass containing different semiconductor nanocrystals [3, 12, 21, 22].

Curve (3) in Fig. 2 represents the absorption spectrum of the oxidized $CuInS_2$ NC sample and consists of an additional broad band in the range of 0.65–1.9 eV and an absorption edge rising from $\sim$ 1.9 eV. This edge is related to the absorption of $CuInS_2$ NC, and there are no noticeable absorption changes in the range of 2.2–3.6 eV after oxidation of the $CuInS_2$ NC. By subtracting the $CuInS_2$ NC absorption curve (1) from that of the oxidized $CuInS_2$ NCs (3), the broad band (4) centered at 1.03 eV has been distinguished as shown by the dotted curve in Fig. 2. This additional absorption band can be attributed to charge transfer in oxidized $Cu^{I}In^{III}S_2^{II}$ NCs containing Cu(II) after thermal oxidation, as observed in oxidized copper sulphide particles [23]. The change of the chemical state of copper in the oxidized $CuInS_2$ NCs studied here has been shown in detail [24] by X-ray photoelectron spectroscopy.

Figure 3 shows the time-dependent ΔOD spectra of the oxidized $CuInS_2$ NC sample. A strong induced absorption

band located at ~ 2.1 eV and an absorption bleaching edge in the range of 1.4–1.7 eV are observed. Figure 4 represents the dynamics of the differential absorption ΔOD at four probe-photon energies E_{probe}. From Figs. 3 and 4, we observe that there are the following spectral and temporal features in behavior of the ΔOD signal: (1) as the pump-probe delay time t_{d} increases, the bleaching edge, defined as the wavelength at which $\Delta OD = 0$, shifts progressively to higher energies (Fig. 3) and eventually reaches ~ 1.7 eV by $t_{\text{d}} \approx 200$ ps (Fig. 4c); the bleaching-edge position obtained after $t_{\text{d}} \approx 200$ ps remains independent of time in the studied time interval (Fig. 4c); (2) the differential absorption signal observed after the 15-ps pump pulse decays to a plateau within about 200 ps; subsequent decay of the differential absorption signal is very slow and estimated to take more than 300 ps. Ultimately, long-lived induced absorption occurs for $E_{\text{probe}} = 1.7$–2.6 eV (Fig. 4a,b), while for $E_{\text{probe}} = 1.4$–1.7 eV, the initial increase in absorption is followed by long-lived bleaching (Fig. 4d). Bleaching is observed in the spectral range corresponding to the high-energy side of the 1.03-eV absorption band of the oxidized $CuInS_2$ NC sample.

3 Discussion

The combination of pump-probe and photoluminescence results leads us to propose an energy-level diagram for oxidized $CuInS_2$ NCs as shown in Fig. 5. In pump-probe experiments, the 1.15-eV pump pulse is tuned inside the absorption band at 1.03 eV (Fig. 2). The 1.03-eV absorption is supposed to originate from a level-A, related to Cu(II) [23], to conduction-band transition (Fig. 5). It should be noted that pumping is tuned outside the excitonic absorption [curve (1) in Fig. 2]. Thus, the pump photon energy is too small to transfer carriers from the valence band to the conduction band (Fig. 5), and the exciton absorption at 1.78 eV does not contribute to the ΔOD spectra observed. When the sample is pumped, carriers are excited from level A to the conduction band, resulting in depletion of level A and corresponding bleaching of the 1.03-eV absorption band. The bleaching in the range of 1.4–1.7 eV observed in the ΔOD spectra is related to the high-energy side of the bleaching of level-A to conduction-band transition. The carriers quickly relax to the bottom of the conduction band or

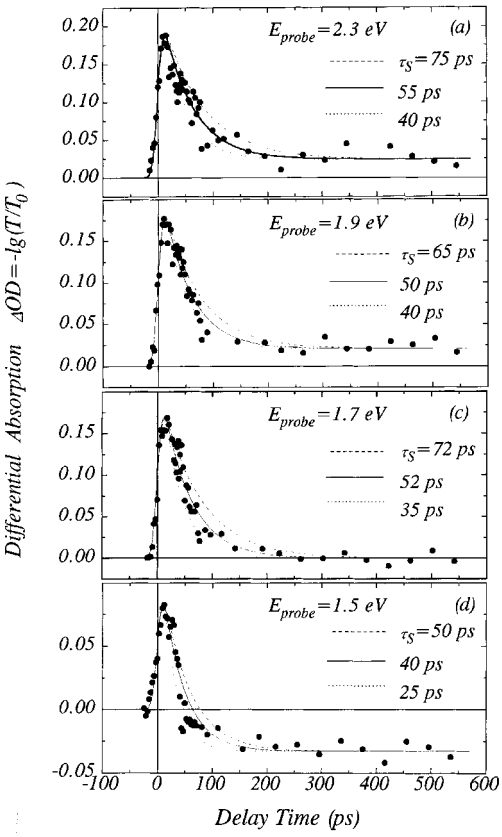

Fig. 4. Differential absorption $\Delta OD = -\lg(T/T_0)$ induced in the oxidized $CuInS_2$ NCs in a PVA film as a function of delay time between pump and probe pulses. The probe-photon energies selected are $E_{\text{probe}} =$ (**a**) 2.3 eV, (**b**) 1.9 eV, (**c**) 1.7 eV, and (**d**) 1.5 eV Experimental data (*points*) obtained with a 15-ps pump pulse at 1.08 μm (1.15 eV) are compared to fits (*curves*) with different values of τ_{S}. The best fits are obtained using $\tau_{\text{S}} =$ **a** 55 ps, **b** 50 ps **c** 52 ps, and **d** 40 ps

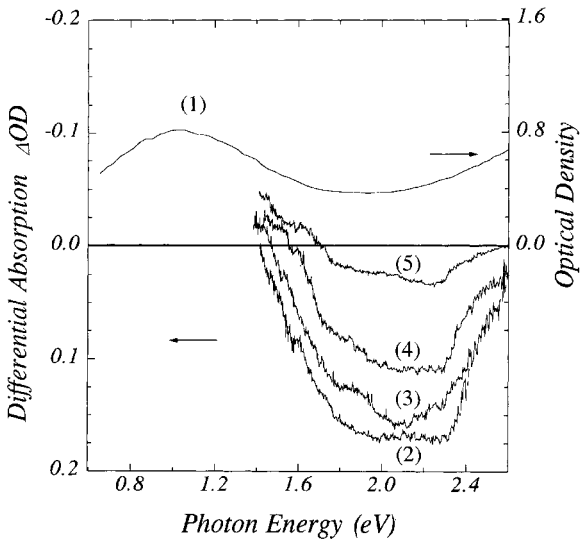

Fig. 3. (1) Linear absorption spectrum of oxidized $CuInS_2$ NCs in a PVA film and (2-5) corresponding differential absorption spectra $\Delta OD = -\lg(T/T_0)$ recorded at different delay times between pump and probe pulses: (2) 11 ps, (3) 38 ps, (4) 52 ps, and (5) 460 ps. A 15-ps pulse at 1.08 μm (1.15 eV) was used as pump

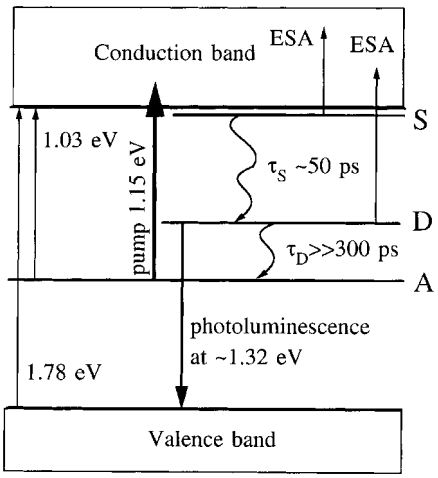

Fig. 5. A schematic energy-level diagram for oxidized $CuInS_2$ NCs based on photoluminescence and picosecond pump-probe results

are captured by the shallow traps (S in Fig. 5) with the energy close to the conduction-band edge. We will consider the latter case since this does not detract from the main features of carrier dynamics that we wish to examine. From level S, the carriers are transferred to deep traps (D in Fig. 5). This level D can be attributed to mid-gap surface states [19, 20] and is responsible for the 1.32-eV photoluminescence observed here [curve (2) in Fig. 2]. The conduction-band to level-S transition occurs on a subpicosecond time scale, and the carriers are transferred to level S within our time resolution of 15 ps. The S-to-D transition has a time constant of ~ 50 ps The lifetime of carriers in deep traps can be estimated at $\gg 300$ ps.

We believe the presence of fast (from level S) and long-lived (from level D) excited-state absorptions (ESAs) in different spectral regions is a likely explanation for the induced absorption and high-energy shift of the bleaching edge observed here. The differential absorption recorded is a combination of three spectra: (1) the level-A to conduction-band bleaching spectrum, (2) the spectrum of ESA from level S, and (3) the spectrum of ESA from level D. Immediately after the pump pulse, level D is empty, and the ESA from level S overcomes the level-A to conduction band transition bleaching in the spectral region examined [curve (2) in Fig. 3]. As the time delay increases, the carriers relax from level S to level D, resulting in an increase in the ESA from level D and a decrease in the ESA from level S. This leads to a modification of the total differential absorption spectrum corresponding to bleaching at its low-energy side [curves (3) and (4) in Fig. 3] because, according to our assumption, the ESAs from level D and level S differ from each other. When all of the excited carriers have relaxed to level D ($t_\mathrm{d} \geq 200$ ps), there is only long-lived ESA from level D. The bleaching of the level-A to conduction-band transition, which remains unchanged after the pump pulse, overcomes the aforementioned ESA in the spectral region of 1.4–1.7 eV [curve (5) in Fig. 3].

In order to find the S-to-D relaxation time τ_S (Fig. 5), we developed a simplified rate-equation model in which, according to the proposed energy-level diagram, the differential absorption signal $\Delta OD(t_\mathrm{d})$ consists of level-A to conduction-band absorption change, ESA from level S, and delayed ESA from level D, and is modeled by three equations:

$$\frac{\mathrm{d}N_\mathrm{S}}{\mathrm{d}t} = \frac{N_0 I_\mathrm{pump}(t)}{\int_{-\infty}^{+\infty} I_\mathrm{pump}(t)\,\mathrm{d}t} - \frac{N_\mathrm{S}}{\tau_\mathrm{S}}\,, \tag{2}$$

$$\frac{\mathrm{d}N_\mathrm{D}}{\mathrm{d}t} = \frac{N_\mathrm{S}}{\sigma_\mathrm{S}}\,, \tag{3}$$

$$\Delta OD(t_\mathrm{d}) \propto \int_{-\infty}^{+\infty} I_\mathrm{probe}(t-t_\mathrm{d})[(\sigma_\mathrm{S}/\sigma_\mathrm{A}-1)N_\mathrm{S}(t) + (\sigma_\mathrm{D}/\sigma_\mathrm{A}-1)N_\mathrm{D}(t)]\,\mathrm{d}t\,, \tag{4}$$

where N_0 is the total excited carrier density, N_S and N_D the time-dependent carrier densities at the excited levels S and D, respectively, $I_\mathrm{probe}(t) = I_\mathrm{pump}(t) = \exp[-(2t/\tau_\mathrm{p})^2]$, τ_p the pulse duration, and σ_A, σ_S, σ_D absorption cross sections from levels A, S, and D, respectively. The values of $\sigma_\mathrm{S}/\sigma_\mathrm{A}$ and $\sigma_\mathrm{D}/\sigma_\mathrm{A}$ are adjustable parameters that depend on the wavelength. We assume that the relaxation time of carriers from D to A is $\tau_\mathrm{D} \gg 300$ ps and the relaxation time from conduction band to S is $\tau_\mathrm{P} < 15$ ps (Fig. 5). Figure 4 shows the comparison of the experimental and calculated $\Delta OD(t_\mathrm{d})$ data at four probe-photon energies E_probe using different values of the relaxation time τ_S. The best fits are obtained using $\tau_\mathrm{S} = 55$ ps, 50 ps, 52 ps, and 40 ps for $E_\mathrm{probe} = 2.3$ eV, 1.9 eV, 1.7 eV, and 1.5 eV, respectively. The differences between the values of τ_S obtained from $\Delta OD(t_\mathrm{d})$ data for different energies E_probe lay within the experimental error of τ_S measurements of $15 \pm$ ps .

4 Conclusion

We have investigated the transient differential absorption spectra of oxidized $CuInS_2$ NCs in a PVA polymer film. The bleaching of an additional absorption band at 1.03 eV which appears in $CuInS_2$ NCs after oxidation and is attributed to charge transfer in oxidized $Cu^{I}In^{III}S_2^{II}$ NCs containing Cu(II) has been observed. The fast-decayed (~ 50 ps) ESA attributing to transition from the shallow traps or bottom of conduction-band as well as long-lived ($\gg 300$ ps) ESA related to the mid-gap surface states have been observed.

Acknowledgements. This work has been granted financial support from the Foundation for Fundamental Research of the Republic of Belarus.

References

1. L.E. Brus: J. Chem. Phys. **79**, 5566 (1983)
2. H. Weller, H.M. Schmitt, U. Koch, A. Fojtik, S. Baral, A. Henglein, W. Kunath, K. Weiss, E. Dieman: Chem. Phys. Lett. **124**, 557 (1986)
3. N.F. Borrelli, D.W. Hall, H.J. Holland, D.W. Smith: J. Appl. Phys. **61**, 5399 (1987)
4. A.P. Alivisatos, T.D. Harris, P.J. Carroll, M.L. Steigerwald, I.E. Brus: J. Chem. Phys. **90**, 3463 (1989)
5. M.G. Bawendi, W.L. Wilson, L. Rothberg, P.J. Caroll, T.M. Jedju, M.L. Steigerwald, L.E. Brus: Phys. Rev. Lett. **65**, 1623 (1990)
6. F. Henneberger, J. Puls, H. Rossmann, U. Woggon, S. Freundt, Ch. Spiegelberg, A. Schulzgen: J. Cryst. Growth **101**, 632 (1990)
7. S.V. Gaponenko, U. Woggon, M. Saleh, W. Langbein, A. Uhrig, M. Muller, C. Klingshirn: J. Opt. Soc. Am. B **10**, 1947 (1993)
8. J. Butty, Y.Z. Hu, N. Peyghambarian, Y.H. Kao, J.D. Mackenzie: Appl. Phys. Lett. **67**, 2672 (1995)
9. N. Sarukura, Y. Ishida, T. Yanagawa, H. Nakano: Appl. Phys. Lett. **57**, 229 (1990)
10. K.V. Yumashev, V.P. Mikhailov, P.V. Prokoshin, S.P. Jmako, I.V. Bodnar: Appl. Phys. Lett. **65**, 2768 (1994)
11. E. Munin, A.B. Villaverde, M. Bass: Opt. Commun. **108**, 278 (1994)
12. Y. Wang, A. Suna, J. Mc Hung, E.F. Hilinski, P.A. Lucas, R.D. Johnson: J. Chem. Phys. **92**, 6927 (1990)
13. H. Yoneyama, T. Torimoto: Adv. Materials **7**, 492 (1995)
14. K.V. Yumashev, P.V. Prokoshin, A.M. Malyarevich, V.P. Mikhailov, M.V. Artemyev, V.S.Gurin: Appl. Phys. B **64**, 73 (1997)
15. S.-H. Wei, A. Zunger: J. Appl. Phys. **78**, 3846 (1995)
16. Y. Kayanuma: Phys. Rev. B **38**, 9797 (1988)
17. R. Marquez, C. Rincon: Phys. Status Solidi **191**,115 (1995)
18. J.L. Shay, J.H. Wernick: *Ternary Chalcopyrite Semiconductors: Growth, Electronic Properties and Application* (Pergamon, Oxford 1975)
19. J. Warnock, D.D. Awschalom: Phys. Rev. B. **32**, 5529 (1985)
20. N. Chestnoy, T.D. Harris, R. Hull, L.E. Brus: J. Phys. Chem. **90**, 3393 (1986)
21. J.P. Zheng, L. Shi, F.S. Choa, P.L. Liu, H.S. Kwok: Appl. Phys. Lett. **53**, 643 (1988)
22. P.A.M. Rodrignes, G. Tamulaitis, P.Y. Yu, S.H. Risbud: *Solid State Commun.* **94**, 583 (1995)
23. E.J. Silvester, F. Grieser, B.A. Sexton, T.W. Healy, *Langmuir* **7**, 2917 (1991)
24. V.S Gurin, V.V. Sviridov, A.S. Lyakhov, E.A. Tyavlovskaya, K.N. Kasparov: Russ. J. Inorg. Chem. **41**, 1(1996)